RESEARCH ARTICLE

Developmental Dynamics WILEY

Anterior patterning genes induced by Zic1 are sensitive to retinoic acid and its metabolite, 4-oxo-RA

Aditi Dubey[1,2] | Jean-Pierre Saint-Jeannet[1] 🟢

[1]Department of Molecular Pathobiology, New York University, College of Dentistry, New York, New York, USA

[2]Alnylam Pharmaceuticals, Cambridge, Massachusetts, USA

Correspondence
Jean-Pierre Saint-Jeannet, Department of Molecular Pathobiology, New York University, College of Dentistry, 345 East 24th Street, New York, NY 10010.
Email: jsj4@nyu.edu

Abstract

Background: Development of paired sensory organs is a highly complex and coordinated process. These organs arise from ectodermal thickenings in the cephalic region known as cranial placodes. We have previously shown that Zic1 is a critical regulator for the formation of the pre-placodal region (PPR), the common territory for the development of all cranial placodes in *Xenopus laevis*.

Results: In this study, we have analyzed a number of Zic1 targets for their expression during PPR patterning, as well as their regulation by retinoic acid (RA) and one of its major metabolites, 4-oxo-RA. Our findings show that anteriorly Zic1 regulates several transcription factors, Crx, Fezf2, Nkx3-1, and Xanf1 as well as a serine/threonine/tyrosine kinase, Pkdcc.2. These factors are all expressed in the vicinity of the PPR and as such are candidate regulators of placode formation downstream of Zic1. In addition to their differential regulation by RA, we find that 4-oxo-RA is also capable of modulating the expression of these genes, as well as a broad array of RA-regulated genes.

Conclusion: Our data highlight the complexity of retinoid-mediated regulation required for Zic1-activated anterior structure specification in *Xenopus*, and the potential physiological role of 4-oxo-RA in cranial placode development.

KEYWORDS
patterning, placode, retinoic acid, *Xenopus*

1 | INTRODUCTION

Cranial placodes are precursors to specialized sense organs in vertebrates that arise from the head ectoderm during embryonic development. They are ectodermal thickenings that are formed at the neural plate border from the common territory, the pre-placodal region (PPR) and subsequently differentiate into placodes with distinct identities, fates, and functions.[1] Cranial placodes give rise to the adenohypophysis, paired sensory organs (the optic lens, the inner ear, and the olfactory epithelium), and sensory cranial ganglia that innervate the orofacial complex.[2] Disruptions in the formation of these placodes often lead to debilitating disorders and malformations such as deafness, blindness, anosmia, hormonal imbalance, and orofacial sensory deficits.

In order to further our understanding of cranial placode development in *Xenopus*, our laboratory has established an animal cap explant assay where the activity of the transcription factor Zic1 was found necessary and sufficient for the expression of PPR genes *six1* and *foxi4.1*.[3] The identification of downstream targets of Zic1 via microarray revealed several genes involved in the retinoic acid (RA) signaling pathway, which is essential for

the noncell autonomous specification of PPR by Zic1.[4] Specifically, the RA synthesizing enzyme RALDH2 and the RA-transporter lipocalin-type prostaglandin D2 synthase that are expressed at the anterior neural plate (ANP) were found to be essential for PPR formation. We further found that the RA-catabolizing enzyme, Cyp26c1, and the RA-dependent transcription factor Pitx2c expressed in a domain between ANP and PPR to be critical for PPR formation.[5] Interestingly, we also discovered that one of the RA metabolites generated by Cyp26c1, 4-oxo-RA, to be present during development at stages critical for the induction and specification of PPR. Consistent with this observation, previous reports have shown that 4-oxo-RA is capable of inducing signaling via RA receptors (RARs) to modulate the development of the anterior-posterior (A-P) axis in the embryo.[6,7]

Given the importance of RA in regulating Zic1 targets in the context of PPR formation, we decided to extend our analysis to additional potential targets to assess their regulation by RA, and by its metabolite 4-oxo-RA. The targets selected for further analysis were screened for their expression in the domains relevant for PPR specification, their regulation by Zic1 and their dependence on RA and 4-oxo-RA treatments. Our findings reveal several additional transcription factors, including Crx, Fezf2, Nkx3-1, and Xanf1, as well as a serine/threonine/tyrosine kinase, Pkdcc.2, that are expressed in the domains adjacent to PPR that are regulated by RA. In addition, we find that 4-oxo-RA is a potent regulator of specification of anterior structures, and of the expression of several Zic1 target genes that are also regulated by RA, suggesting that 4-oxo-RA is capable of playing an important role in the specification of PPR. This is a significant new finding given that RA metabolites are typically thought to be biologically inactive and cleared from the cell in which they are produced. This work has the potential to transform our understanding of RA regulation and function during embryogenesis.

2 | RESULTS

2.1 | Key anterior patterning genes are expressed during PPR formation

A microarray screen conducted to identify targets of Zic1 yielded several genes known for their patterning functions in other model systems.[4] We selected for genes highly up-regulated by Zic1 and narrowed our choices based on expression profiling data available in Xenbase (xenbase.org), and previously published reports documenting a role for these genes in A-P patterning or

development in general. These parameters yielded five candidate genes for further analysis, several of which are transcription factors: *crx/otx5b* is known to be involved in eye development,[8] *fezf2* is a known regulator of neuronal development,[9] *nkx3-1* has as yet undefined roles in early development but may function in sclerotome development,[10,11] and *xanf1/hesx1* is important for the development of anterior forebrain across species, including *Xenopus*.[12,13] Interestingly, *pkdcc.2*, which is a kinase, was also identified as a Zic1 target and regulates the Wnt/planar cell polarity (PCP) pathway in *Xenopus*.[14] These genes are collectively referred to as "Zic1 targets" henceforth.

Zic1 has been shown to be a key regulator of the formation of the PPR. Therefore, to further investigate the potential role of these genes in this Zic1-driven pathway, we performed in situ hybridization (ISH) to visualize the spatiotemporal expression of these genes during early embryonic development. Figure 1 shows that these Zic1 targets are expressed during gastrulation (Nieuwkoop and Faber [NF] stages 10–13) and their domain of expression narrows as development progresses through neurulation (NF stages 15–17). Importantly, *fezf2* and *xanf1* appear to be expressed in the ANP, whereas *nkx3-1* is expressed in the PPR-adjacent domain ventral to the ANP, where it overlaps with the anterior domain of *crx*. *pkdcc.2* shows a broader expression pattern that includes the neural fold as well as the ANP (see Table 1 for a summary of gene expression). Taken together, this analysis reveals that the Zic1 targets are expressed at temporal stages and in spatial domains relevant to PPR formation, either overlapping with or adjacent to the ANP Zic1-expression domain.

2.2 | Patterning genes are targets of Zic1

We next sought to verify that Zic1 is required for the expression of these genes. Using a well-characterized Zic1 morpholino antisense oligonucleotides (Zic1MO[3-5,15]), we knocked down Zic1 in one half of the embryo at the two-cell stage and assessed the consequences by ISH at NF stage 15 (Figure 2). Our analysis revealed that Zic1 knockdown indeed disrupted the expression of these genes, providing further evidence that they are Zic1 targets. Loss of Zic1 resulted mostly in the expansion of the expression domains for *crx*, *fezf2*, *pkdcc.2*, and *xanf1*, whereas *nkx3-1* expression was significantly reduced. Pitx2c, a previously identified Zic1 target[5] was also reduced. These results validate our microarray findings and establish Zic1 as a potent regulator of the above targets.
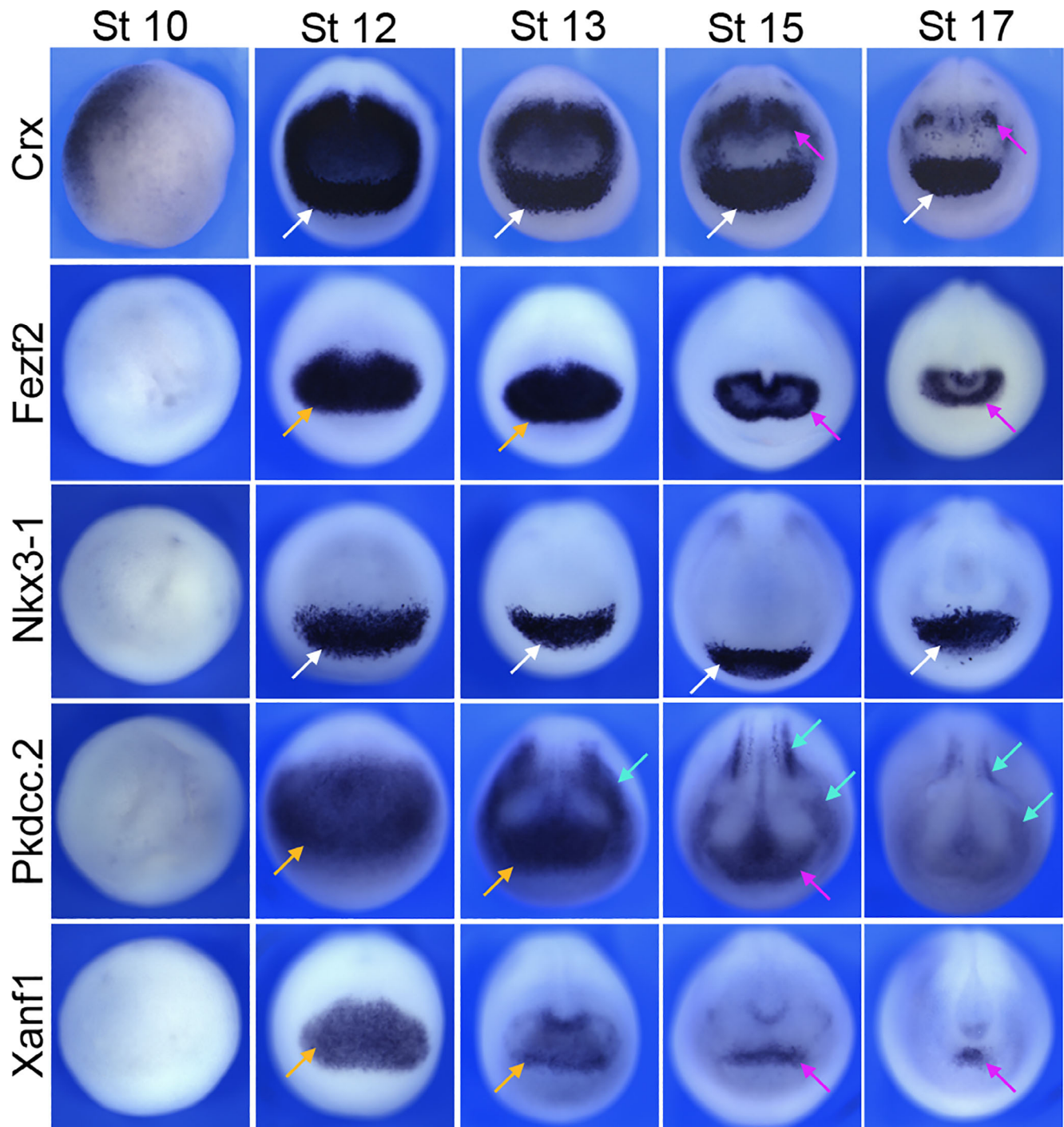
FIGURE 1   Key patterning genes are expressed in the vicinity of the pre-placodal region (PPR) and Zic1 expression domain. In situ hybridization (ISH) for *crx*, *fezf2*, *nkx3-1*, *pkdcc.2*, and *xanf1* (top to bottom) expression across developmental stages from gastrula to neurula stages. Nieuwkoop and Faber (NF) stages are indicated on top of each row. All panels are anterior views with dorsal to the top. Anterior neural plate: orange arrows; PPR-adjacent domain: white arrows; anterior neural fold: purple arrows; neural crest domain: green arrows. For a summary of the domain of expression, see Table 1

2.3 | Zic1 induces patterning genes in an RA-dependent manner

To further validate if the Zic1 targets participate in the PPR formation pathway through RA signaling, we used animal cap explants to investigate their activation under conditions where RA signaling is blocked. As seen in Figure 3, applying disulfiram (DSF), a broad inhibitor of RA synthesis,[16,17] to animal cap explants expressing Zic1 (Zic1GR[3]) abrogated the activation of all Zic1 targets

TABLE 1 Summary of the developmental expression of Zic1 targets

Gene name	Anterior neural plate	PPR-adjacent domain	Anterior neural fold	Dorsal neural fold/neural crest domain
crx	−	+	+	−
fezf2	+	−	+	−
nkx3-1	−	+	−	−
pkdcc.2	+	−	+	+
xanf1	+	−	+	−

Note: + expressed; − not detected.

Abbreviation: PPR, pre-placodal region.

(Figure 3). The result for *nkx3-1* was not as consistent, suggesting a more complex regulation mechanism (Figure 3C). Altogether, these data demonstrate that Zic1 regulates these genes indirectly through RA signaling.

2.4 | Patterning genes respond to both RA and 4-oxo-RA

Further assessment of the impact of RA signaling on the expression of Zic1 targets was performed through dose-response experiments. Given our previous findings that *Xenopus* embryos contain a significant amount of the RA metabolite, 4-oxo-RA,[5] we wanted to determine if 4-oxo-RA is capable of regulating the expression of Zic1 targets. 4-oxo-RA is one of the polar metabolites generated by the action of Cyp26 enzymes on all-trans RA[18-20]; however, the extent of its biological activity, if any, has been debated.

To determine whether 4-oxo-RA induces changes in the overall A-P axis specification in developing *Xenopus* embryos similar to those seen with RA,[21-23] NF stage 11 embryos were treated with increasing doses of 4-oxo-RA (Figure 4) and the dorsoanterior index (DAI) was measured at NF stage 34. DAI is a scale developed to assess axis defects in *Xenopus* embryos, based on whether ventralization or dorsalization has occurred.[24] Briefly, a DAI grade between 0 and 10 is assigned based on the phenotype whereby an embryo with DAI 5 represents a normal embryo, DAI 0 being the most ventroposteriorized with no head or axial structures, and DAI 10 being the most dorsoanteriorized with only head structures that are radially symmetrical (Figure 4B[24]). Upon treatment with increasing doses of 4-oxo-RA, embryos display posteriorization with the majority of embryos exhibiting head truncations akin to DAI 2 and 3 (Figure 4A,C). This is consistent with a previous report showing that 4-oxo-RA has axis posteriorizing activity.[6]

Next, we assessed the gene expression changes in Zic1 targets induced by RA and 4-oxo-RA in parallel. Figure 5 shows the summary findings of changes in gene expression of *crx*, *fezf2*, *nkx3-1*, *pkdcc.2*, and *xanf1*. We have previously shown that *pitx2c* and *hnf1b* show decreasing and increasing expression, respectively, upon treatment with increasing RA doses[5] and they serve as positive controls for the treatments. Our analysis reveals 4-oxo-RA as not only capable of regulating the expression of Zic1 targets, but that the effect of 4-oxo-RA is very similar to that of RA, albeit at a higher dose (Figure 4, compare 1 μM RA and 10 μM 4-oxo-RA). These findings suggest that Zic1 targets are sensitive to RA levels and demonstrate that the RA metabolite, 4-oxo-RA has biological signaling activity and regulates the expression of Zic1 targets in a manner similar to RA.

2.5 | RNA-sequencing reveals broad similarities in gene activation between RA and 4-oxo-RA

The discovery that 4-oxo-RA regulates the expression of patterning genes similarly to RA prompted us to use next-generation sequencing to determine the extent to which the two retinoids bring about similar changes in gene expression. We subjected anterior halves of *Xenopus* embryos to RA or 4-oxo-RA treatment mid-gastrulation (NF stage 12.5) and analyzed the global changes in RNA expression at NF stage 15 (Figure 6A). Heat map analysis of the top 50 differentially regulated genes by RA (Figure 6B) and 4-oxo-RA (Figure 6C) showed gene expression changes in known RA-target genes, as well as several novel genes. Further examination revealed that several of the highly up-regulated genes between RA and 4-oxoRA were identical, such as *cyp26a1*, *cyp26c1*, *dhrs3*, *hoxa1*, *ripply3*, and *znf703* (Figure 6D,E). Zic1 targets were also identified in these data (Table 2), with the magnitude of gene expression change (represented by $\log_2$ fold change) correlating with loss or expansion of expression observed in Figure 5. The only exception was *nkx3-1*, which was not detected in the 4-oxo-RA vs dimethylsulfoxide (DMSO) data set (see Section 3). Altogether, these data further validate that Zic1 targets are regulated similarly by both RA and 4-oxoRA, consistent with the whole embryo immersion experiments above (Figure 5).

To determine the extent to which the gene expression changes induced by the two retinoids overlap, Venn diagram comparisons between RA vs DMSO and 4-oxo-RA vs DMSO were made (Figure 6F,G). Interestingly, the majority of the genes up-regulated by 4-oxo-RA were also up-regulated by RA, whereas the majority of genes down-
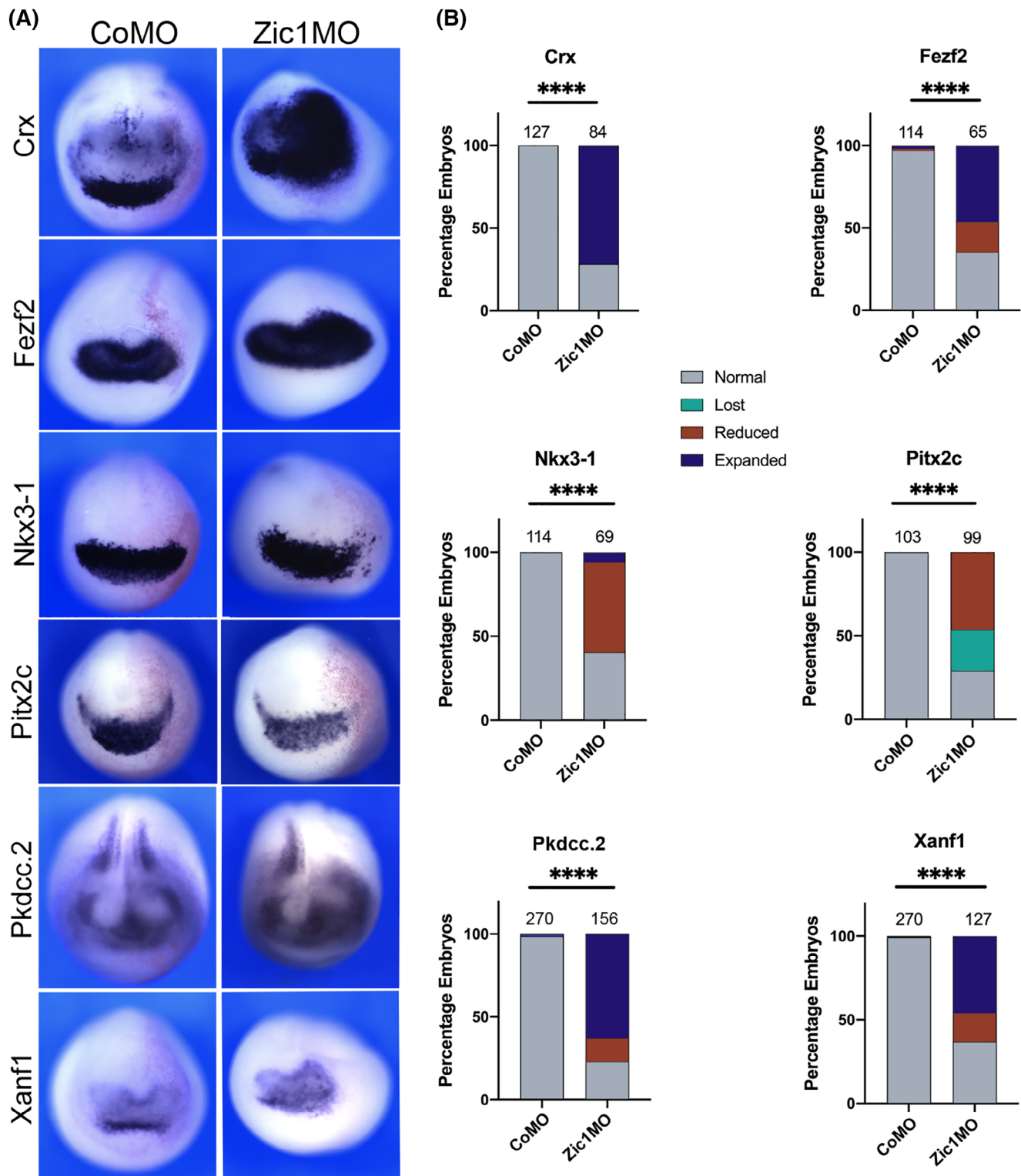
FIGURE 2 *crx*, *fezf2*, *nkx3-1*, *pkdcc.2*, and *xanf1* are targets of Zic1. (A) In situ hybridization (ISH) for *crx*, *fezf2*, *nkx3-1*, *pkdcc.2*, and *xanf1* (top to bottom) in control (CoMO) and Zic1 morpholino antisense oligonucleotide (Zic1MO)-injected Nieuwkoop and Faber (NF) stage 15 embryos. Representative images are shown, with the injected side on the right. All panels are anterior views with dorsal to the top. (B) Frequency of the phenotypes. The number of embryos analyzed for each condition is on the top of each bar; *P* values were calculated using Chi-squared test, ****$P < .0001$
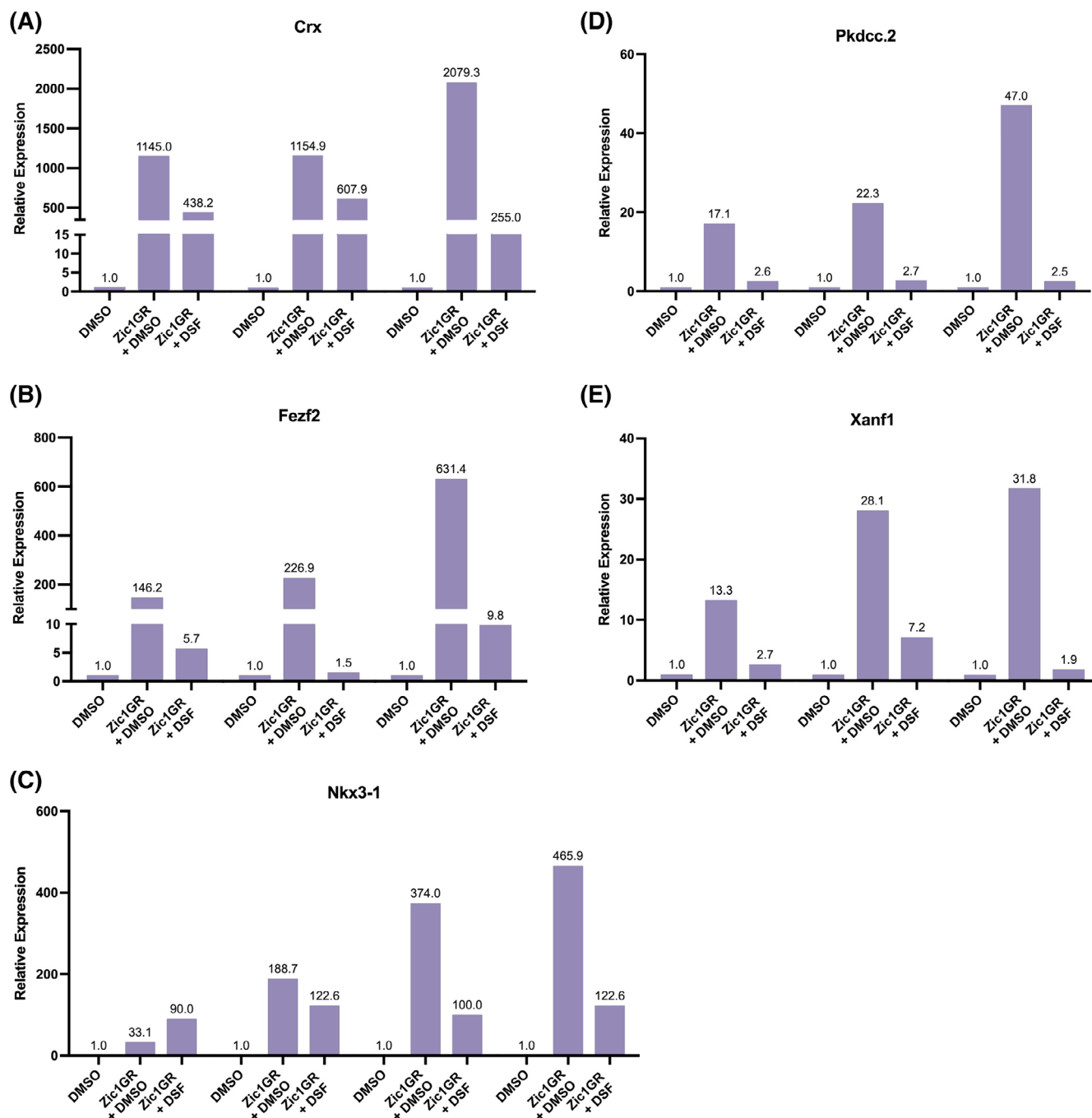
FIGURE 3 Induction of Zic1 targets is dependent on retinoic acid (RA) synthesis. real-time quantitative polymerase chain reaction (qRT-PCR) analysis of *crx* (A), *fezf2* (B), *nkx3-1* (C), *pkdcc.2* (D), and *xanf1* (E) expression in Zic1GR-injected animal cap explants cultured for 8 hours in the presence of dexamethasone with or without disulfiram (DSF; 100 μM). Three (A-E) and four (C) biological replicates are shown. Expression levels are normalized to ODC with fold change in relative expression indicated at the top of each bar

regulated by RA were not down-regulated by 4-oxo-RA. Despite these differences, a significant overlap in common genes was observed in both the up-regulated and down-regulated data sets (see Table 3 for the top 20 genes). Gene ontology (GO) analyses identified several terms pertaining to A-P axis specification, placode formation, and neural crest development were enriched in the embryos exposed to RA and 4-oxo-RA (Figure 6H,I). Particularly, ectodermal placode formation was enriched in genes up-regulated by RA and 4-oxo-RA, and A-P pattern specification was enriched in genes down-regulated in both conditions. Taken together, these results demonstrate that globally, the genes expression changes induced by 4-oxo-RA are highly similar to those induced by RA,
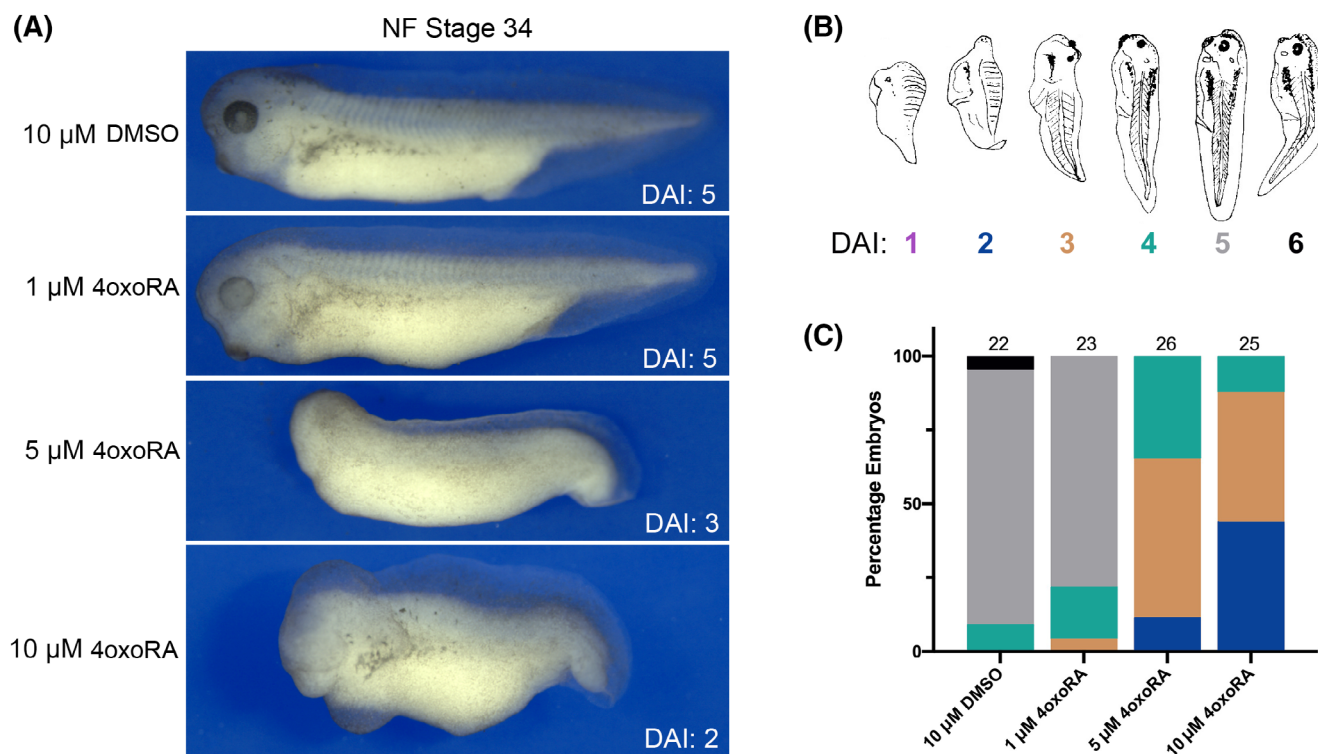
FIGURE 4 4-oxo-RA causes posteriorization of the embryo axis. (A) Brightfield images of *Xenopus* Nieuwkoop and Faber (NF) stage 34 embryos treated at NF stage 11 with either 10 μM dimethylsulfoxide (DMSO) or increasing doses of 4-oxo-RA as shown. All panels are lateral views with dorsal to the top and anterior to the left. (B) Schematic representation of the dorsoanterior index (DAI) assignments is as defined previously.[24] (C) Frequency of DAI phenotypes of 4-oxo-RA-treated embryos. Total embryos analyzed per condition are indicated at the top of the bar

lending credence to 4-oxo-RA's ability to act as a morphogen during development.

3 | DISCUSSION

This study highlights the complexity of morphogens that operate during cranial placode development, and broadly, during the development of anterior structures in the *Xenopus* embryo. In our previous work,[4,5] we elucidated an RA-dependent program of cranial placode specification executed by Zic1. In this study, we have further defined the extent of this regulation by characterizing several Zic1 targets that are expressed in the ANP or the PPR-adjacent domain. In addition, we followed up on our previous observation that the RA metabolite, 4-oxo-RA, is present at high levels in the developing *Xenopus* embryo[5] to show that 4-oxo-RA is in fact capable of extensive gene expression regulation in a manner similar to RA. Our findings point to 4-oxo-RA as an active morphogen during embryonic development, further suggesting that gradients established during embryonic development cannot be fully explained by a "source and sink" model.[25,26]

3.1 | Zic1 targets are RA-dependent patterning genes

Several Zic1 targets expressed in these domains are genes with predicted or defined roles in embryonic development, further validating Zic1's role as a key regulator of developmental processes involved in head formation through modulation of RA. Crx (also known as otx5b) has been shown to be critical for photoreceptor development in the retina.[27,28] Fezf2 is an important regulator of forebrain development, and more specifically, of projection neurons in the mammalian neocortex, as well as monoaminergic neurons[2,29,30]

On the other hand, while several members of the NKX gene family have been shown to play key roles during development,[31] the role of *nkx3-1* is less clear. Reports in mice have shown *nkx3-1* to be involved in sclerotome development,[11] minor salivary glands and prostate duct morphogenesis.[32] Interestingly, in *Xenopus*, *crx*, *nkx3-1*, and *pitx2c* were strongly induced by *pitx1*, a gene that is also expressed in the PPR-adjacent domain.[33] The study also suggested that while the induction of *crx* and *nkx3-1* appears direct, the induction of *pitx2c* is likely indirect. This finding is especially intriguing in light of our
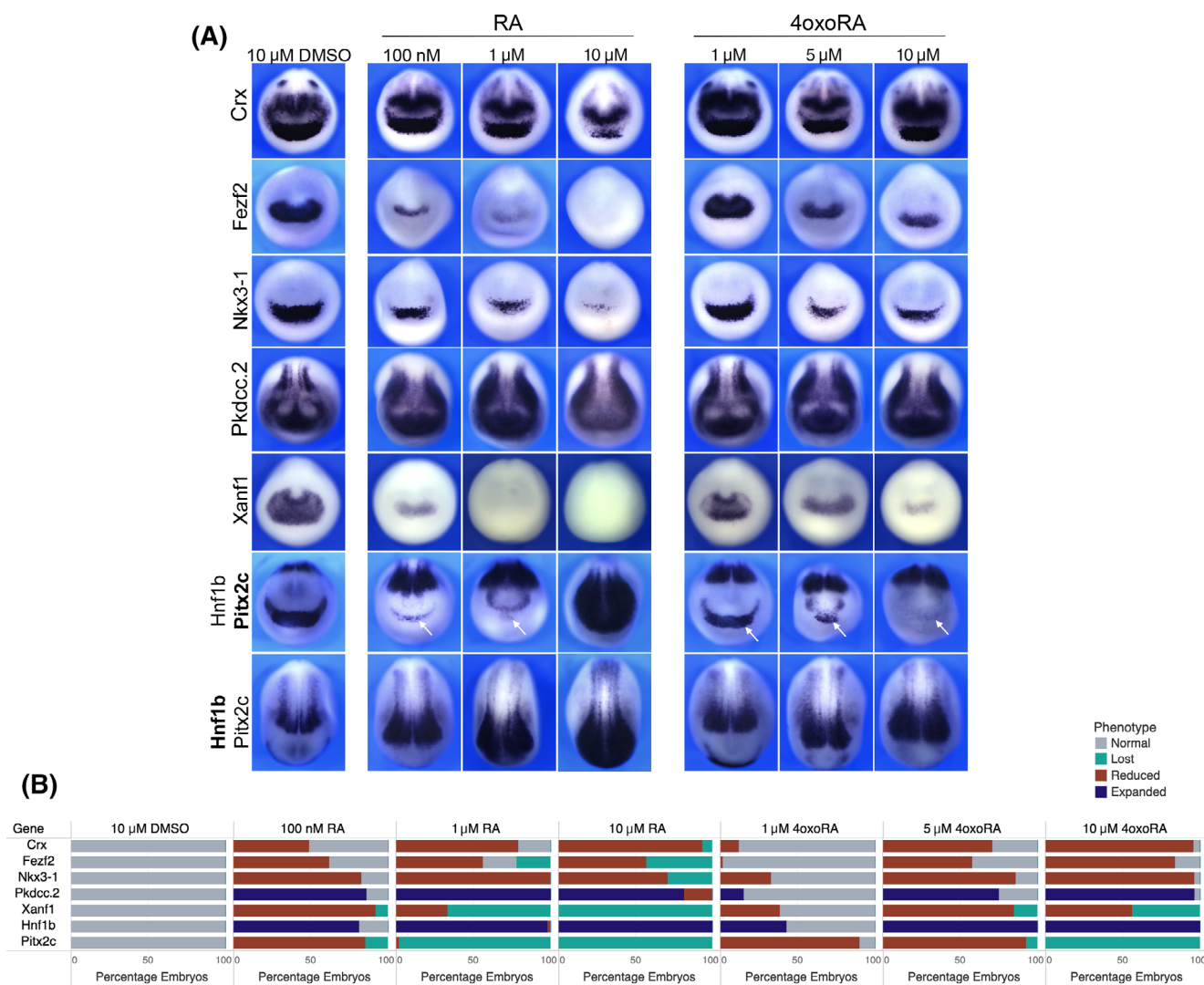
FIGURE 5 Zic1 targets show sensitivity to both retinoic acid (RA) and 4-oxo-RA. (A) In situ hybridization (ISH) for *crx*, *fezf2*, *nkx3-1*, *pkdcc.2*, and *xanf1* expression on stage 15 embryos treated with either 10 μM dimethylsulfoxide (DMSO) or increasing doses of RA (left) or 4-oxo-RA (right) as shown. Bottom two rows show *pitx2c* and *hnf1b* as controls in a double ISH where the gene considered is indicated in bold, ***pitx2c*** (middle row) and ***hnf1b*** (bottom row), respectively. White arrows indicate position of the pre-placodal region (PPR)-adjacent domain of *pitx2c*. All images show anterior views with dorsal to top, except for *hnf1b*, where dorsal views are presented with anterior to bottom. (B) Frequency of phenotypes with n ≥ 50 embryos per condition from two biological replicates

previous work showing *pitx2c* as a Zic1 target[5] and our microarray analysis that identified *pitx1* as a Zic1 target, however, at levels approximately half that of *pitx2c* (data not shown). In future work, it will be interesting to elucidate the relationship between these genes, and we speculate that these interactions might contribute to the variability of *nkx3-1* induction levels in response to Zic1GR expression (Figure 3).

Xanf1 (also known as hesx1) is perhaps the best-characterized gene in embryonic development, though its regulation by Zic1 has not been previously described. Xanf1 functions during forebrain development to regulate formation of the anterior neuroectoderm in mice[12]

and *Xenopus*,[34] where it acts as a transcriptional repressor. Mutations in human *Hesx1* gene have been reported to cause septo-optic dysplasia,[35] an early forebrain development disorder presenting with hypoplasia of the optic nerves, midline brain defects, as well as pituitary-related deficiencies.[36]

Out of the five Zic1 targets presented in this study, *pkdcc2* is the only gene that is not a transcription factor.[14] *pkdcc.2* is one of two *Xenopus* homologs of the mouse and human *Pkdcc* gene, encoding a secreted tyrosine kinase.[37] *Pkdcc* knockdown in mice has been shown to result in a host of defects, including short limbs and cleft palate.[38] In *Xenopus*, *pkdcc.2* and *pkdcc.1* have been
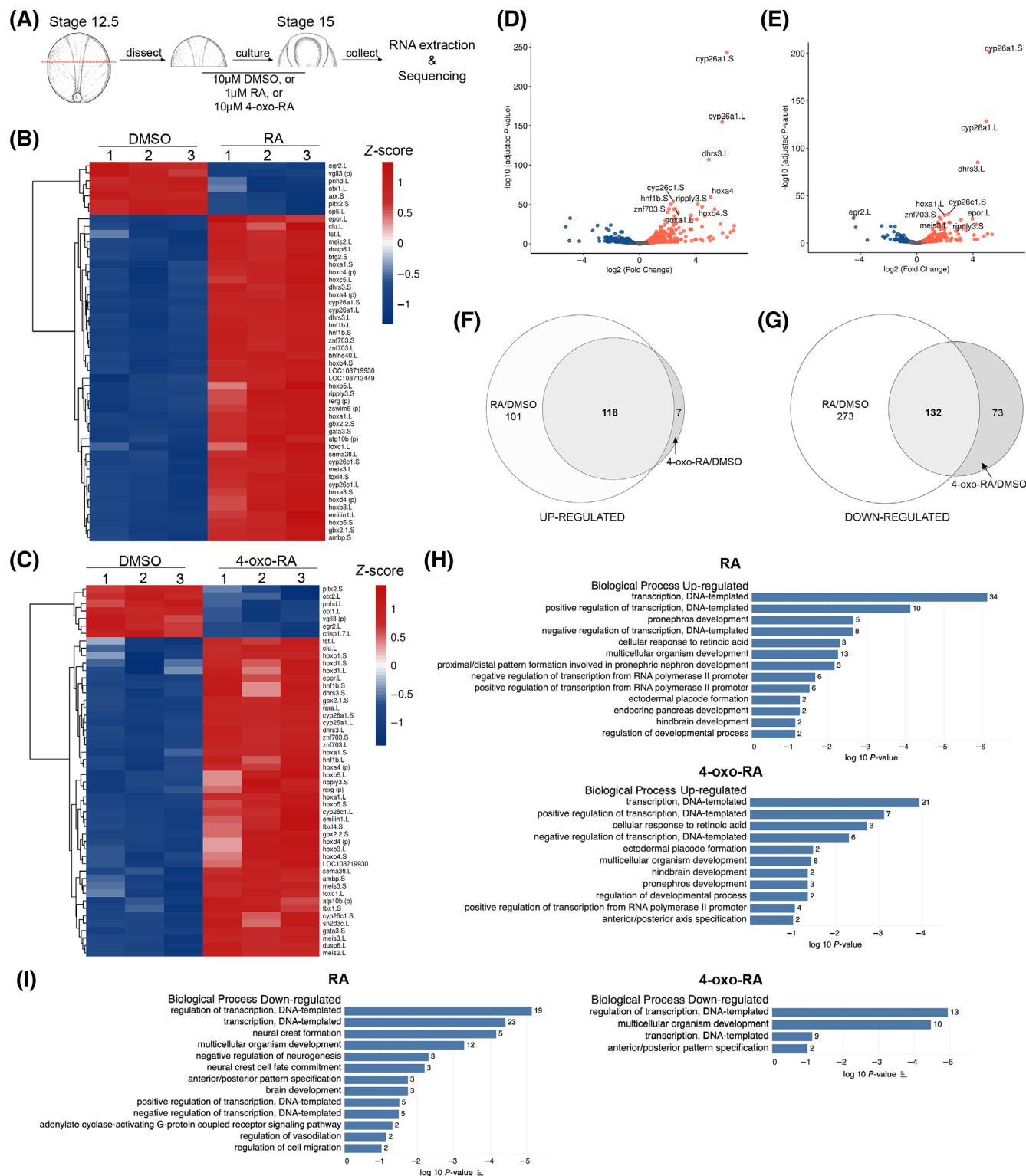
FIGURE 6 RNA-sequencing (RNA-Seq) analysis reveals similarities in genes regulated by retinoic acid (RA) and 4-oxo-RA. (A) Schematic of experimental design for RNA-Seq analysis. (B) Heatmap analysis showing the top 50 differentially expressed genes based on pairwise comparison of normalized count matrix between 10 μM dimethylsulfoxide (DMSO) and 1 μM RA-treated anterior embryo halves. (C) Heatmap analysis of the top 50 differentially expressed genes between 10 μM DMSO and 10 μM 4-oxo-RA-treated anterior embryo halves, similarly analyzed as (B). Heatmaps were colored by z-score. (D) Volcano plots showing significance of differential gene expression on *y*-axis (log$_{10}$ adjusted *P* value) vs magnitude of differential gene expression on *x*-axis (log$_2$ fold change) for 10 μM DMSO vs 1 μM RA-treated anterior halves, with the top 10 genes labeled with their Xenbase ID. (E) Volcano plot similarly analyzed as (D) showing top 10 differentially regulated genes for 10 μM DMSO vs 10 μM 4-oxo-RA-treated anterior halves, with top 10 genes with their Xenbase ID. Venn diagram analysis for genes up-regulated (F) or down-regulated (G) upon RA and 4-oxoRA treatments. Gene ontology (GO) analysis using DAVID Bioinformatics Resources was performed for genes up-regulated by RA (H, top) and 4-oxo-RA (H, bottom). GO analysis for genes down-regulated by RA (I, left) and 4-oxo-RA (I, right)

TABLE 2   Magnitude of gene expression change

Zic1 target	Log$_2$ fold change RA vs DMSO	Log$_2$ fold change 4-oxoRA vs DMSO
Crx	−1.24	−0.53
Fezf2	−1.43	−0.64
Nkx3-1	−0.56	Not identified
Pkdcc.2	0.62	0.63
Xanf1	−2.09	−1.13
Hnf1b	2.44	1.96
Pitx2c	−2.04	−1.62

Note: Fold change (log$_2$ fold change) observed for Zic1 targets in the RNA-Seq analysis. Positive fold changes represent up-regulated genes, whereas down-regulated genes show negative log$_2$ fold change.
Abbreviations: DMSO, dimethylsulfoxide; RA, retinoic acid; RNA-seq, RNA-sequencing.

TABLE 3   Top 20 common genes up-regulated and down-regulated by retinoic acid (RA) and 4-oxo-RA

Common genes up-regulated	Common genes down-regulated
hoxb5.S	*vgll3 (p)*
cyp26b1.L	*egr2.L*
LOC494794	*arx.S*
hoxb6.L	*pnhd.L*
cyp26a1.L	*trpm1 (p)*
hoxd4.L	*barhl2.S*
hoxa4 (p)	*otx1.L*
akr1c2.S	*crisp1.7.L*
dhrs3.L	*wnt8b (p)*
epor.L	*sp5.L*
hoxb4.S	*dmrta1.S*
clu.L	*Xelaev18032865m*
ripply3.S	*sst.1.S*
rerg (p)	*nog2.S*
cd69 (p)	*hesx1.L*
LOC108701043	*nrp1.S*
LOC108697667	*XB5848002.L*
tlx3 (p)	*rspo2.L*
bhlhe40.L	*twist1.S*
hoxb3.L	*wnt8b.S*

Note: The genes are ranked by fold change from high to low. (p) provisional name.

shown to regulate blastopore and neural tube closure through regulation of the Wnt-PCP signaling pathway,[14] highlighting *pkdcc.2*'s role as a patterning gene during embryonic development. With the exception of *nkx3-1*,

blocking RA signaling through DSF causes reduction in gene expression of these Zic1 target genes, indicating that they are involved in the Zic1-activated pathway that is critical for cranial placode specification.[5] Future studies will examine the functional role of these genes in cranial placode specification.

3.2 | 4-oxo-RA is an active morphogen during *Xenopus* development

Another important finding of this study is the demonstration that 4-oxo-RA is an important morphogen capable of inducing gene expression changes in *Xenopus* embryos similar to RA. Based on genetic evidence, it has been proposed that retinoid metabolites do not regulate development[39]; however, this study did not specifically assess the effect of any metabolite on gene expression of RA targets. Our approach involved directly treating the embryo with 4-oxo-RA during the "RA sensitivity" window[40] to assess if any morphological defects or gene expression changes could be observed. Indeed, we observe A-P defects in 4-oxo-RA treated embryos (Figure 4) consistent with previous results.[6] In addition, we observed quantifiable changes in known RA target genes, both through ISH experiments and RNA-sequencing (RNA-seq) analyses (as detailed later).

Although changes in gene expression upon exogenous treatment of embryos with RA or 4-oxo-RA may not necessarily reflect an endogenous role for these molecules, this approach still provides meaningful information on their potential activity. Prior to this work, two studies have examined 4-oxo-RA in *Xenopus* embryonic development, but this work presents the first investigation of 4-oxo-RA activity at a global level in the embryo. It was previously shown that 4-oxo-RA is capable of interacting with RARs with almost similar affinity as RA for RARα, but with significantly higher affinity for RARβ and RARγ.[41] This work along with our prior study[5] demonstrated that 4-oxo-RA levels could be measured in *Xenopus* embryos at consistently higher levels than RA, suggesting that it may be the major retinoid species in frogs. However, it is unclear whether these levels of 4-oxo-RA are due to maternal accumulation, or generated specifically for signaling during embryonic development as a consequence of Cyp26 enzymes RA catabolizing activity.[5] In addition, we have previously shown that cranial placode formation via Zic1 does not require RARs.[4] It will be interesting to see which receptors are responsible for retinoid signaling for placode specification, and subsequently, if 4-oxo-RA has a higher affinity for this receptor and can compete with RA.

The genes identified in our RNA-seq analysis were specifically enriched for anterior structures by only analyzing the anterior half of the embryo. This also allowed us to exclude gene expression changes resulting from interactions with the second major source of RA in the embryo, the paraxial mesoderm.[42] As seen in Figure 6, the majority of genes up-regulated by 4-oxo-RA are also up-regulated by RA, albeit at a lower dose. These genes including *dhrs3*, *cyp26a1*, *hoxd4*, *hoxa1*, *hnf1b*, and so on are known RA-responsive genes and have previously been identified in screens for RA targets,[43] demonstrating that 4-oxo-RA is an active retinoid in the *Xenopus* embryo. Interestingly, with the exception of *nkx3-1*, all Zic1-targets characterized in this study were also identified in the RNA-seq (see Table 2) with similar up- or down-regulation trends as observed in Figure 5. In this analysis, *nkx3-1* did not reach the threshold of adjusted *P* value <.05. This could be due to the fact that the embryos analyzed via RNA-seq were treated with the respective retinoids for a shorter period of time (from NF stages 12.5 to 15; Figure 6) as compared to the whole embryo treatment (from NF stages 11 to 15; Figure 5). It is worth noting that despite the similarities in the pathways up- or down-regulated by RA and 4-oxo-RA, the impact of RA is greater, with over 600 differentially regulated genes that span a greater range of biological processes than 4-oxo-RA (Figure 6). Based on these data, we conclude that while 4-oxo-RA is capable of inducing similar gene expression changes, 4-oxo-RA affects fewer targets than RA.

Overall, our results demonstrate that the presence of Cyp26 enzymes in a particular domain adjacent to an RA synthesizing domain does not necessarily serve as a "sink," as the metabolites generated have biological activity. We speculate that this might indicate a role of 4-oxo-RA as a "backup" mechanism, where in the event of excess RA degradation, crucial genes may still be activated. Alternatively, it may be a remnant of maternal RA deposits in the yolk that accumulates over time and can perform essential gene activation in the absence of sufficient RA. Consistent with previous reports[44,45] we also find that 4-oxo-RA induces *cyp26a1* and *cyp26c1* expression, raising the interesting possibility that these enzymes are also needed to further oxidize the metabolites 4-oxo-RA, 18-OH-RA, and 4-OH-RA, as seen for human Cyp26c1.[46] While it has been shown that 4-oxo-RA can bind to RARs[41] and alter the expression of genes known to contain RA response elements (RAREs), it is also possible that it is regulating gene expression in a RARs-independent manner, based on cellular and tissue context. These are important questions that require further investigation to understand the physiological function for 4-oxo-RA during development.

4 | EXPERIMENTAL PROCEDURES

4.1 | Plasmids and oligonucleotides

Xenopus laevis Zic1GR and the tracer β-galactosidase mRNAs were synthesized using the Message mMachine SP6 and T7 Transcription kits (Ambion, SP6 Cat# AM1340; T7 Cat# AM1344) as described previously.[5] A well-characterized Zic1MO[3-5,15] was purchased from GeneTools (Philomath, OR). A standard control morpholino (CoMO) was used as control.

4.2 | Embryos, injections, treatments, and animal cap explant culture

As described by Dubey et al, *X. laevis* embryos were staged according to Nieuwkoop and Faber[47] and raised in 0.1X Normal Amphibian Medium (NAM).[48] All experiments in this study were conducted in accordance with the guidelines of the Guide for the Care and Use of Laboratory Animals of the National Institutes of Health. All protocols requiring *Xenopus* were approved by the Institutional Animal Care and Use Committee of New York University under animal protocol #IA16-00052. In microinjection experiments, embryos were injected in one blastomere at the two-cell stage (NF stage 2) and collected at NF stage 15 for ISH. An amount of 40 to 60 ng of MO or CoMO and 0.5 ng of *β-galactosidase* mRNA as a lineage tracer were used in injections. CoMO-injected embryos were used as controls. RA (all-trans RA, Sigma-Aldrich, Cat# R2625) and 4-oxo-RA (Sigma-Aldrich, Cat#07558) treatments were performed using stock solutions prepared in DMSO (Sigma-Aldrich Cat# D8418). NF stage 11 embryos were incubated in RA diluted in 0.1X NAM (100 nM, 1 μM, 10 μM) or 4-oxo-RA diluted in 0.1X NAM (1 μM, 5 μM, 10 μM) and collected at NF stage 15 for ISH (Figure 5) or NF stage 34 (Figure 4). Anterior halves of the embryos used in Figure 6 were treated at NF stage 12.5 and collected at NF stage 15. Sibling embryos treated with 10 μM DMSO served as controls.

For animal cap explant assays, one blastomere of a two-cell stage embryo was injected in the animal pole region with 250 pg Zic1GR mRNA, as previously described.[4] The explants were dissected at the blastula stage (NF stage 9) and culture in 0.5X NAM with 10 μM dexamethasone (Sigma-Aldrich, Cat# D1756) for 8 hours at 24°C unless otherwise noted, then collected and immediately stored at −80°C. DSF of 100 μM (tetraethylthiuram disulfide, Sigma-Aldrich, Cat# 86720) was added to the incubation medium for DSF-treated caps. All experiments were performed on at least three independent batches of embryos (obtained from three

separate females). For whole embryo treatment and injection experiments, 50 embryos per injection and per marker were used, and 12 to 15 animal caps per condition were used in animal cap explant assays.

4.3 | In situ hybridization

ISH was performed as previously described.[5,49,50] Briefly, NF stage 15 embryos were fixed in 0.1 M MOPS (4-Morpholinepropanesulfonic acid sodium salt), 2 mM EGTA (ethylene glycol-bis(2-aminoethyl ether)-N,N,N′, N′-tetraacetic acid), 1 mM $MgSO_4$ and 3.7% formaldehyde for 1 hour. Red-Gal (Research Organics, Cat#C40040) staining was performed prior to ISH when β-galactosidase mRNA was used as tracer. No tracers were used in RA and 4-oxoRA immersion experiments.

Whole-mount ISH was performed in 4-mL glass vials on a standard bench top nutator. *crx*, *fezf2*, and *nkx3-1* (purchased form OpenBiosystems; ThermoFisher Scientific, Waltham, Massachusetts), *hnf1b*[51] and *pitx2c*[52] digoxygenin (DIG)-labeled antisense RNA probes were synthesized using the Genius Kit (Roche, Cat#1175025). To generate *pkdcc.2* and Xanf1 probes, *pkdcc.2* and *xanf1* sequences were amplified from *X. laevis* NF Stage 12 cDNA and cloned into pGEMT-Easy (Promega, Cat#A1360), and linearized templates were used to synthesize the corresponding DIG-labeled probes.

Hybridization was performed overnight at 60°C. For the detection of RNA probes, the embryos were incubated with an anti-DIG antibody conjugated to alkaline phosphatase (Roche, Cat#11093274910; 1:2000 dilution) overnight at 4°C. Several successive washes were used for excess antibody removal and the chromogenic reaction performed overnight at room temperature in BM purple (Roche, Cat#11442074001). The embryos were subsequently bleached in 10% hydrogen peroxide in methanol for 48 hours and subsequently imaged in 1X phosphate-buffered saline.

4.4 | RNA-sequencing

Extracted total RNA from anterior halves of NF stage 15 embryos was verified on the Agilent Bioanalyzer system using a nanochip to verify the RNA integrity number. High-quality total RNA (500 ng) was input into the Illumina Truseq v2 stranded mRNA library prep kit (Cat#20020595) according to the manufacturer's protocol. Generated cDNA was amplified with 12 polymerase chain reaction (PCR) cycles. Final generated libraries were verified on the Agilent Tapestation 2200 system using high-sensitivity DNA Screentape. Sample concentration was checked on the Invitrogen qubit system using the high-sensitivity DNA reagent. Each sample was normalized to a specific nanomolar concentration and pooled equally into a final combined pool. The pool was run on one lane of Novaseq SP100 flow cell (run length was 50 paired-end bases) on the Illumina Novaseq 6000 sequencing system.

4.5 | Bioinformatics analysis

RNA-seq data were analyzed by sns rna-star pipeline (https://igordot.github.io/sns/routes/rna-star.html). Adapters and low-quality bases were trimmed using Trimmomatic (v0.36).[53] Sequencing reads were mapped to the reference genome (XENLA_9.2, http://www. xenbase.org/common/displayJBrowse.do?data=data/xl9_ 2) using the STAR aligner (v2.7.3).[54] Alignments were guided by a Gene Transfer Format (GTF) file, which was converted from a General Feature Format file. The mean read insert sizes and their SDs were calculated using Picard tools (v.2.18.20) (http://broadinstitute.github.io/ picard). The gene-samples counts matrix was generated using featureCounts (v1.6.3),[55] normalized based on their library size factors using DEseq2,[56] and differential expression analysis was performed.

The read per million (RPM) normalized BigWig files were generated using deepTools(v.3.1.0).[57] To compare the level of similarity among the samples and their replicates, we used two methods: principal-component analysis and Euclidean distance-based sample clustering. All the downstream statistical analyses and plot generation were performed in R environment (4.0.3; https://www.r-project.org/). Significant testing was done using Wald Chi-squared test and the Benjamini-Hochberg procedure was used to generate adjusted *P* values that were used as inputs for Volcano plot analysis of differential gene expression. GO enrichment analyses were performed using DAVID Bioinformatics Resources 6.8.[58,59]

4.6 | Real-time quantitative PCR analysis

Total RNA was extracted from 12 to 15 animal cap explants using the RNeasy Micro kit (Qiagen, Cat# 74004) and quantified using a Nanodrop spectrophotometer (Nanodrop Technologies). Genomic DNA was removed by on-column digestion with RNase-free DNase I for 15 minutes at room temperature. Ten nanogram of total RNA was used per reaction. Real-time quantitative PCR (qRT-PCR) was performed using the One-Step RT-PCR kit (Applied Bioystems, Cat# 4388869, 4389988).

The mean Ct value for each biological replicate was calculated from four technical replicates. The primers used for qRT-PCR are listed below.

Gene	Forward primer	Reverse primer
pkdcc.2	5′-GGACAGTTCCCAAT GACTTCT-3′	5′-GTGACGCTAGAGG GCTTATTT-3′
xanf1	5′-AGAGAGAAC TGAGCTGGTA TAGG-3′	5′-GGATAGGAA TTCACTCGGA ACAC-3′
nkx3-1	5′-AGGTCATAGAGCTG GAAAGAAAG-3′	5′-AGGCTCTTG GCAAGCTG-3′
crx	5′-CAAACCCACGGAA ACAAAGAAG-3′	5′-GCACTCGGGATTCT GGTAAAT-3′
fezf2	5′-GTCTGCGGA AAGGTGTTTAATG-3′	5′-CGTGTGGATGATCT TGTGTCT-3′
ODC	5′-ACATGGCATTCTCC CTGAAG-3′	5′-TGGTCCCAA GGCTAAAGTTG-3′

4.7 | Imaging

Embryos processed for ISH were imaged using a dual light-fluorescence Leica M165 Stereomicroscope, with the same exposure and magnification used for each marker in the experiment. Representative images of the dominant phenotype were captured and the image panels were composed using Adobe Photoshop.

4.8 | Statistical analysis

Unless otherwise stated, experiments were conducted in embryos from three or more female *Xenopus* for biological replicates. No prior analysis was done to calculate the sample size. As previously described,[5] to assess changes in expression of the genes of interest, Zic1MO-injected embryos were compared to CoMO-injected embryos, and for each unilaterally injected embryo the injected side was compared to the uninjected side as well, for an additional internal control. Each embryo was assigned one of the following phenotypes: normal, lost or reduced, expanded, or ectopic. For RA/4-oxo-RA-treated embryos, the treated embryos were compared with DMSO-treated controls at an equivalent dose and assigned phenotypes as above. For whole-mount ISH experiments, the data from all biological replicates were pooled for statistical analysis, and significance testing was performed using the Chi-squared test using GraphPad Prism 9 (GraphPad Software). $P < .05$ was considered significant, unless otherwise stated. For animal cap qRT-PCR experiments,

three or four biological replicates are provided in Figure 3. Data in Figure 5 were visualized using Tableau (Tableau Software).

CONFLICT OF INTEREST
The authors declare no potential conflict of interest.

AUTHOR CONTRIBUTIONS
Aditi Dubey: Conceptualization (equal); data curation (lead); formal analysis (equal); investigation (equal); methodology (equal); visualization (lead); writing – original draft (lead). **Jean-Pierre Saint-Jeannet:** Conceptualization (equal); funding acquisition (lead); investigation (supporting); project administration (lead); resources (supporting); supervision (lead); writing – review and editing (equal).

DATA AVAILABILITY STATEMENT
All data supporting the results are available from the corresponding author upon request. The RNA-seq data have been deposited onto GEO under accession number: GSE180269.

ORCID
Jean-Pierre Saint-Jeannet https://orcid.org/0000-0003-3259-2103

REFERENCES
1. Saint-Jeannet J-P, Moody SA. Establishing the pre-placodal region and breaking it into placodes with distinct identities. *Dev Biol.* 2014;389(1):13-27. https://doi.org/10.1016/j.ydbio.2014.02.011

2. Schlosser G. Making senses: development of vertebrate cranial placodes. In: Jeon K, ed. *International Review of Cell and Molecular Biology*. Vol 283. San Diego, CA: Academic Press; 2010: 129-234. https://doi.org/10.1016/S1937-6448(10)83004-7

3. Hong C-S, Saint-Jeannet J-P. The activity of Pax3 and Zic1 regulates three distinct cell fates at the neural plate border. *Mol Biol Cell*. 2007;18(6):2192-2202. https://doi.org/10.1091/mbc.e06-11-1047

4. Jaurena MB, Juraver-Geslin H, Devotta A, Saint-Jeannet J-P. Zic1 controls placode progenitor formation non-cell autonomously by regulating retinoic acid production and transport. *Nat Commun*. 2015;6:7476. https://doi.org/10.1038/ncomms8476

5. Dubey A, Yu J, Liu T, Kane MA, Saint-Jeannet J-P. Retinoic acid production, regulation and containment through Zic1, Pitx2c and Cyp26c1 control cranial placode specification. *Development*. 2021;148(4):1-14. https://doi.org/10.1242/dev.193227

6. Pijnappel WWM, Hendriks HFJ, Folkers GE, et al. The retinoid ligand 4-oxo-retinoic acid is a highly active modulator of positional specification. *Nature*. 1993;366:340-344. https://doi.org/10.1038/366340a0

7. Achkar CC, Derguini F, Blumberg B, et al. 4-Oxoretinol, a new natural ligand and transactivator of the retinoic acid receptors. *Proc Natl Acad Sci*. 1996;93(10):4879-4884. https://doi.org/10.1073/pnas.93.10.4879

8. Whitaker SL, Knox BE. Conserved transcriptional activators of the *Xenopus* rhodopsin gene. *J Biol Chem*. 2004;279(47):49010-49018. https://doi.org/10.1074/jbc.M406080200

9. Chen B, Schaevitz LR, McConnell SK. Fezl regulates the differentiation and axon targeting of layer 5 subcortical projection neurons in cerebral cortex. *Proc Natl Acad Sci USA*. 2005; 102(47):17184-17189. https://doi.org/10.1073/pnas.0508732102

10. Tanaka M, Lyons GE, Izumo S. Expression of the Nkx3.1 homeobox gene during pre and postnatal development. *Mech Dev*. 1999;85(1):179-182. https://doi.org/10.1016/s0925-4773(99)00084-2

11. Herbrand H, Pabst O, Hill R, Arnold H-H. Transcription factors Nkx3.1 and Nkx3.2 (Bapx1) play an overlapping role in sclerotomal development of the mouse. *Mech Dev*. 2002;117(1): 217-224. https://doi.org/10.1016/s0925-4773(02)00207-1

12. Martinez-Barbera JP, Rodriguez TA, Beddington RS. The homeobox gene Hesx1 is required in the anterior neural ectoderm for normal forebrain formation. *Dev Biol*. 2000;223(2): 422-430. https://doi.org/10.1006/dbio.2000.9757

13. Andoniadou CL, Signore M, Young RM, et al. HESX1- and TCF3-mediated repression of Wnt/β-catenin targets is required for normal development of the anterior forebrain. *Development*. 2011;138(22):4931-4942. https://doi.org/10.1242/dev.066597

14. Vitorino M, Silva AC, Inácio JM, et al. Xenopus Pkdcc1 and Pkdcc2 are two new tyrosine kinases involved in the regulation of JNK dependent Wnt/PCP signaling pathway. *PLoS One*. 2015;10(8):e0135504. https://doi.org/10.1371/journal.pone.0135504

15. Sato T, Sasai N, Sasai Y. Neural crest determination by co-activation of *Pax3* and *Zic1* genes in *Xenopus* ectoderm. *Development*. 2005;132(10):2355-2363. https://doi.org/10.1242/dev.01823

16. Kitson TM. The effect of disulfiram on the aldehyde dehydrogenases of sheep liver. *Biochem J*. 1975;151(2):407-412. https://doi.org/10.1042/bj1510407

17. Veverka KA, Johnson KL, Mays DC, Lipsky JJ, Naylor S. Inhibition of aldehyde dehydrogenase by disulfiram and its metabolite methyl diethylthiocarbamoyl-sulfoxide. *Biochem Pharmacol*. 1997;53(4):511-518. https://doi.org/10.1016/s0006-2952(96)00767-8

18. White JA, Beckett-Jones B, Guo YD, et al. cDNA cloning of human retinoic acid-metabolizing enzyme (hP450RAI) identifies a novel family of cytochromes P450. *J Biol Chem*. 1997; 272(30):18538-18541. https://doi.org/10.1074/jbc.272.30.18538

19. White JA, Ramshaw H, Taimi M, et al. Identification of the human cytochrome P450, P450RAI-2, which is predominantly expressed in the adult cerebellum and is responsible for all-trans-retinoic acid metabolism. *Proc Natl Acad Sci USA*. 2000; 97(12):6403-6408. https://doi.org/10.1073/pnas.120161397

20. Taimi M, Helvig C, Wisniewski J, et al. A novel human cytochrome P450, CYP26C1, involved in metabolism of 9-cis and all-trans isomers of retinoic acid. *J Biol Chem*. 2004;279(1):77-85. https://doi.org/10.1074/jbc.M308337200

21. Katsuyama Y, Saiga H. Retinoic acid affects patterning along the anterior-posterior axis of the ascidian embryo. *Dev Growth Differ*. 1998;40(4):413-422. https://doi.org/10.1046/j.1440-169x.1998.t01-2-00006.x

22. Grandel H, Lun K, Rauch G-J, et al. Retinoic acid signalling in the zebrafish embryo is necessary during pre-segmentation stages to pattern the anterior-posterior axis of the CNS and to induce a pectoral fin bud. *Development*. 2002;129(12):2851-2865. https://doi.org/10.1242/dev.129.12.2851

23. Dubey A, Rose RE, Jones DR, Saint-Jeannet J-P. Generating retinoic acid gradients by local degradation during craniofacial development: one cell's cue is another cell's poison. *Genesis*. 2018;56(2):e23091. https://doi.org/10.1002/dvg.23091

24. Kao KR, Elinson RP. The entire mesodermal mantle behaves as Spemann's organizer in dorsoanterior enhanced *Xenopus laevis* embryos. *Dev Biol*. 1988;127(1):64-77. https://doi.org/10.1016/0012-1606(88)90189-3

25. Crick F. Diffusion in embryogenesis. *Nature*. 1970;225(5231): 420-422. https://doi.org/10.1038/225420a0

26. Shimozono S, Iimura T, Kitaguchi T, Higashijima S-I, Miyawaki A. Visualization of an endogenous retinoic acid gradient across embryonic development. *Nature*. 2013;496(7445): 363-366. https://doi.org/10.1038/nature12037

27. Vignali R, Colombetti S, Lupo G, et al. Xotx5b, a new member of the Otx gene family, may be involved in anterior and eye development in *Xenopus laevis*. *Mech Dev*. 2000;96(1):3-13. https://doi.org/10.1038/nature12037

28. Shen Y-C, Raymond PA. Zebrafish cone-rod (crx) homeobox gene promotes retinogenesis. *Dev Biol*. 2004;269(1):237-251. https://doi.org/10.1016/j.ydbio.2004.01.037

29. Shimizu T, Hibi M. Formation and patterning of the forebrain and olfactory system by zinc-finger genes Fezf1 and Fezf2. *Dev Growth Differ*. 2009;51(3):221-231. https://doi.org/10.1111/j.1440-169X.2009.01088.x

30. Zhang S, Li J, Lea R, Vleminckx K, Amaya E. Fezf2 promotes neuronal differentiation through localised activation of Wnt/β-catenin signalling during forebrain development. *Development*. 2014;141(24):4794-4805. https://doi.org/10.1242/dev.115691

31. Stanfel MN, Moses KA, Schwartz RJ, Zimmer WE. Regulation of organ development by the NKX-homeodomain factors: an NKX code. *Cell Mol Biol*. 2005;(Suppl 51):Ol785-Ol799.

32. Schneider A, Brand T, Zweigerdt R, Arnold H-H. Targeted disruption of the Nkx3.1 gene in mice results in morphogenetic defects of minor salivary glands: parallels to glandular duct morphogenesis in prostate. *Mech Dev*. 2000;95(1):163-174. https://doi.org/10.1016/s0925-4773(00)00355-5

33. Jin Y, Weinstein DC. Pitx1 regulates cement gland development in *Xenopus laevis* through activation of transcriptional targets and inhibition of BMP signaling. *Dev Biol*. 2018;437(1): 41-49. https://doi.org/10.1016/j.ydbio.2018.03.008

34. Ermakova GV, Alexandrova EM, Kazanskaya OV, Vasiliev OL, Smith MW, Zaraisky AG. The homeobox gene, Xanf-1, can control both neural differentiation and patterning in the presumptive anterior neurectoderm of the *Xenopus laevis* embryo. *Development*. 1999;126(20):4513-4523. https://doi.org/10.1242/dev.126.20.4513

35. Dattani MT, Martinez-Barbera J-P, Thomas PQ, et al. Mutations in the homeobox gene HESX1/Hesx1 associated with septo-optic dysplasia in human and mouse. *Nat Genet*. 1998; 19(2):125-133. https://doi.org/10.1038/477

36. Webb EA, Dattani MT. Septo-optic dysplasia. *European Journal of Human Genetics*. 2010;18(4):393-397. https://doi.org/10.1038/ejhg.2009.125

37. Bordoli MR, Yum J, Breitkopf SB, et al. A secreted tyrosine kinase acts in the extracellular environment. *Cell*. 2014;158(5): 1033-1044. https://doi.org/10.1016/j.cell.2014.06.048

38. Imuta Y, Nishioka N, Kiyonari H, Sasaki H. Short limbs, cleft palate, and delayed formation of flat proliferative chondrocytes in mice with targeted disruption of a putative protein kinase gene, Pkdcc (AW548124). *Dev Dyn*. 2009;238(1):210-222. https://doi.org/10.1002/dvdy.21822

39. Niederreither K, Abu-Abed S, Schuhbaur B, Petkovich M, Chambon P, Dollé P. Genetic evidence that oxidative derivatives of retinoic acid are not involved in retinoid signaling during mouse development. *Nat Genet*. 2002;31:84-88. https://doi.org/10.1038/ng876

40. Cunningham ML, Mac Auley A, Mirkes PE. From gastrulation to neurulation: transition in retinoic acid sensitivity identifies distinct stages of neural patterning in the rat. *Dev Dyn*. 1994; 200(3):227-241. https://doi.org/10.1002/aja.1002000305

41. Blumberg B, Bolado J, Derguini F, et al. Novel retinoic acid receptor ligands in *Xenopus* embryos. *Proc Natl Acad Sci USA*. 1996;93(10):4873-4878. https://doi.org/10.1073/pnas.93.10.4873

42. Molotkova N, Molotkov A, Sirbu IO, Duester G. Requirement of mesodermal retinoic acid generated by Raldh2 for posterior neural transformation. *Mech Dev*. 2005;122(2):145-155. https://doi.org/10.1016/j.mod.2004.10.008

43. Arima K, Shiotsugu J, Niu R, et al. Global analysis of RAR-responsive genes in the *Xenopus neurula* using cDNA microarrays. *Dev Dyn*. 2005;232(2):414-431. https://doi.org/10.1002/dvdy.20231

44. Topletz AR, Tripathy S, Foti RS, Shimshoni JA, Nelson WL, Isoherranen N. Induction of CYP26A1 by metabolites of retinoic acid: evidence that CYP26A1 is an important enzyme in the elimination of active retinoids. *Mol Pharmacol*. 2015;87(3): 430-441. https://doi.org/10.1124/mol.114.096784

45. Idres N, Marill J, Flexor MA, Chabot GG. Activation of retinoic acid receptor-dependent transcription by all-trans-retinoic acid metabolites and isomers. *J Biol Chem*. 2002;277(35):31491-31498. https://doi.org/10.1074/jbc.M205016200

46. Zhong G, Ortiz D, Zelter A, Nath A, Isoherranen N. CYP26C1 is a hydroxylase of multiple active retinoids and interacts with cellular retinoic acid binding proteins. *Mol Pharmacol*. 2018; 93(5):489-503. https://doi.org/10.1124/mol.117.111039

47. Nieuwkoop PD, Faber J. *Normal Table of Xenopus laevis (Daudin)*. North-Holland Publishing Co; Garland Publishing; 1967.

48. Slack JM, Forman D. An interaction between dorsal and ventral regions of the marginal zone in early amphibian embryos. *J Embryol Exp Morphol*. 1980;56:283-299.

49. Harland RM. In situ hybridization: an improved whole-mount method for *Xenopus* embryos. *Methods Cell Biol*. 1991;36:685-695. https://doi.org/10.1016/s0091-679x(08)60307-6

50. Saint-Jeannet J-P. Whole-mount in situ hybridization of *Xenopus* embryos. *Cold Spring Harbor Protocols*. 2017;2017(12): pdb.prot097287. https://doi.org/10.1101/pdb.prot097287

51. Demartis A, Maffei M, Vignali R, Barsacchi G, De Simone V. Cloning and developmental expression of LFB3/HNF1 beta transcription factor in *Xenopus laevis*. *Mech Dev*. 1994;47(1):19-28. https://doi.org/10.1016/0925-4773(94)90092-2

52. Jeong Y-HP, Park B-K, Saint-Jeannet J-P, Lee Y-H. Developmental expression of Pitx2c in *Xenopus* trigeminal and profundal placodes. *Int J Dev Biol*. 2014;58:701-704. https://doi.org/10.1387/ijdb.140254js

53. Bolger AM, Lohse M, Usadel B. Trimmomatic: a flexible trimmer for Illumina sequence data. *Bioinformatics*. 2014;30(15): 2114-2120. https://doi.org/10.1093/bioinformatics/btu170

54. Dobin A, Davis CA, Schlesinger F, et al. STAR: ultrafast universal RNA-seq aligner. *Bioinformatics*. 2012;29(1):15-21. https://doi.org/10.1093/bioinformatics/bts635

55. Liao Y, Smyth GK, Shi W. featureCounts: an efficient general purpose program for assigning sequence reads to genomic features. *Bioinformatics*. 2013;30(7):923-930. https://doi.org/10.1093/bioinformatics/btt656

56. Love MI, Huber W, Anders S. Moderated estimation of fold change and dispersion for RNA-seq data with DESeq2. *Genome Biol*. 2014;15(12):550. https://doi.org/10.1186/s13059-014-0550-8

57. Ramírez F, Ryan DP, Grüning B, et al. deepTools2: a next generation web server for deep-sequencing data analysis. *Nucleic Acids Res*. 2016;44(W1):W160-W165. https://doi.org/10.1093/nar/gkw257

58. da Huang W, Sherman BT, Lempicki RA. Systematic and integrative analysis of large gene lists using DAVID bioinformatics resources. *Nat Protoc*. 2009;4(1):44-57. https://doi.org/10.1038/nprot.2008.211

59. Huang da W, Sherman BT, Lempicki RA. Bioinformatics enrichment tools: paths toward the comprehensive functional analysis of large gene lists. *Nucleic Acids Res*. 2009;37(1):1-13. https://doi.org/10.1093/nar/gkn923